Morphodynamics of the Qiantang Estuary, China: Controls of river flood events and tidal bores

Xie, Dongfeng; Pan, Cunhong; Gao, Shu; Wang, Zhengbing

DOI
10.1016/j.margeo.2018.09.003

Publication date
2018

Document Version
Accepted author manuscript

Published in
Marine Geology

Citation (APA)
Xie, D., Pan, C., Gao, S., & Wang, Z. (2018). Morphodynamics of the Qiantang Estuary, China: Controls of river flood events and tidal bores. *Marine Geology*, *406*, 27-33. https://doi.org/10.1016/j.margeo.2018.09.003

Morphodynamics of the Qiantang Estuary, China: Controls of river flood events and tidal bore

Dongfeng Xie[1], Cunhong Pan[1], Shu Gao[2], Zheng Bing Wang[3,4]

[1]Zhejiang Institute of Hydraulics and Estuary, Hangzhou, China.

[2]State Key Laboratory for Estuarine and Coastal Research, East China Normal University, Shanghai, China.

[3]Faculty of Civil Engineering and Geosciences, Delft University of Technology, The Netherlands.

[4]Deltares, P.O. Box 177, 2600 MH Delft, The Netherlands.

Corresponding author: Dongfeng Xie (dongfeng.xie@hotmail.com).

Highlights:

- Qiantang Estuary shows strong seasonal and inter-annual morphological changes.
- The tidal bore transports sediment landward and plays an important role for the long-term morphological evolution.
- A power function has been found between the high river discharge and channel volume of the upper estuary.
- Dynamic equilibrium is maintained by high river discharge and the flood-dominant tide.

Abstract

The importance of seasonal variations in river discharge on the morphological development of estuaries has been recognized in recent years, yet *in situ* observations about such variations are rare. Here we report a long-term dataset of bathymetry in the Qiantang Estuary, characterized by the presence of a large-scale sediment deposit system and tidal bore. Moreover, a hydrographic survey of the bore dynamics was carried out covering a spring-neap tidal cycle in 2015. Meanwhile, detailed seasonal bathymetric data together with daily river discharge of 2015 were collected. The morphology shows strong seasonal and inter-annual variations. During high flow season, the river flow erodes the bed and transports a large amount of sediments seaward. A good power function exists between the high river discharge and the channel volume at the upper estuary. Flood tides dominate under usual flow discharge condition. In particular, the tidal bore during spring and intermediate tides which is characterized by large current velocity and suspended sediment concentration, transports a large amount of sediment landward. Over a year, a dynamic morphological equilibrium can be maintained. The estuary has also been significantly influenced by the large-scale embankment in last decades, which constrained the lateral migration of thalweg, bank erosion and point bar deposition, which usually occurs in natural sinuous estuaries.

Key words: Morphodynamic equilibrium; river discharge; tidal asymmetry; tidal bore; Qiantang Estuary; Hangzhou Bay.

1. Introduction

Estuaries are defined as semi-enclosed coastal bodies of water which have free connection with the open sea (Fairbridge, 1980). They are among the most important interfaces on earth. They provide navigation channels, ports, land resources, conditions for recreational activities, and so on. They also play an important role in global carbon / biogeochemical cycling, and provide habitats for flora and fauna. Estuaries are fairly ephemeral features at the geological time scale and frequently influenced by natural changes and human interventions (e.g. Dyer, 1995; Savenije, 2005). From the management point of view, it is of major significance to understand and predict the sediment transport and morphological evolution in estuaries.

Morphological evolution in an estuary is controlled by the nonlinear interactions among hydrodynamics, sediment transport and bed level changes (e.g. Dyer, 1995; Hibma et al., 2004; Dalrymple and Choi, 2007). A morphological equilibrium can be reached when erosion and deposition balance over a long enough time span (e.g. Lanzoni and Seminara, 2002; Hoitink et al., 2017). In recent years, many numerical models have found that an equilibrium state of tidal channel morphology can be reached asymptotically, normally assuming that the river discharge can be ignored or be a constant (e.g. Lanzoni and Seminara, 2002; van der Wegen and Roelvink, 2008; Yu et al., 2012; Bolla Pittaluga et al., 2015). On the other hand, it has been recognized that seasonal variations of river discharge play an important role on the morphological development of estuaries (e.g. Cooper, 2002; Savenije, 2005; Shaw and Mohrig, 2014; Zhang et al., 2016). Recently, Hoitink et al (2017) proposed a conceptual model that in the case of a near-equilibrium, sediment import during low flows can balance sediment export during high flow over a seasonal cycle. It would be valuable to offer a better illustration of such concept, using a time series of morphological data from a real estuary.

Sediment deposit, one of the most important morphological features within an estuary, can form when the estuary received sufficient sediment supply (Dyer, 1995; Dalrymple and Choi, 2007; Gao and Collins, 2014). One typical example is the large subaqueous deposit in the upper and middle reaches of the Qiantang Estuary, China. It starts at about 80 km from the mouth, extends by about 130 km longitudinally, and has a height of 10 m above the baseline at the top of the deposit (Fig. 1). Based on sedimentological surveys, it has been revealed that the sediment of this large sedimentary system is from the adjacent Changjiang River (Chien et al., 1964; Chen et al., 1990; Zhang et al., 2015). Recent modeling by Xie et al (2017a) found that the deposits would grow unlimitedly under normal discharge condition due to the continuous sediment import by flood dominance, and the growth can be constrained by high discharge. Xie et al (2017b) also analyzed the morphological response of the Qiantang Estuary-Hangzhou Bay system to the reduction of sediment load from the adjacent Changjiang Estuary and the large-scale embankment within the estuary. However, few field data have been reported on the morphological equilibrium, leaving a gap between the sediment transport and morphological evolution because of the lack of observed hydrological data.

The Qiantang Estuary is strongly influenced by the river flood events and tidal bore. In addition, the estuary is mainly composed of fine sediment that can be easily resuspended and transported. As a result, the estuary is characterized by active morphological changes on seasonal and inter-annual time scales. In this study, we analyze the seasonal and long-term morphodynamic evolutions of the bar in the Qiantang Estuary, quantify the roles of the flood events and the tidal bore and explore the underlying physical mechanisms for the dynamic equilibrium.

2. Study area

The Qiantang Estuary is located on the coast of the East China Sea (Fig.1a). It is 282-km long convergent estuary, with the width decreasing from 98.5 km at the mouth to less than 1 km at the landward end. The upper 75 km reach from Fuchun power station (FPS) to Zakou is dominated by river flow, the middle reach of 122 km (from Zakou to Ganpu) is controlled by both the river flow and tides, while the lower reach of 85 km (downstream of Ganpu), also well known as Hangzhou Bay, is dominated by tidal currents (Han et al., 2003). The middle and upper reaches of the estuary is overwhelmed by a large longitudinal sediment deposit that elongated from Zapu in the middle of Hangzhou Bay to about 130 km upstream. The bed level rises gradually from 10 m below mean sea level (MSL) to 1 m above MSL and then lowers to more than 10 m below MSL (Fig. 1b).

The tidal wave deforms rapidly landward due to estuarine convergence and shallowing water depth. The mean tidal range increases upstream from about 3.2 m at the mouth, with the maximum of 6 m at Ganpu, and then gradually decreases landward. The tidal wave evolves into a tidal bore at Yanguan section. It is the largest in the world, with the averaged bore height being 1-2 m and the maximum exceeding 3 m (Bartsch-Winkler and Lynch, 1988; Pan et al., 2007; Chanson, 2012).

The annual mean discharge of the Qiantang River is 952 m^3/s. Due to the monsoon climate, the river discharge shows a clear seasonal variation: the low discharge occurs from August to next March and the high discharge occurs from April to July. It also varies on the inter-annual time scale, with sometimes continuous high or low flow years (Han et al., 2003).

Sediment in the Qiantang Estuary is mainly composed of fine and well-sorted silt and clay, with the median grain size between 20 to 40 μm, mainly dispersed from the adjacent Changjiang Estuary (Milliman et al., 1985; Chen et al., 1990).

Since the 1960s, a large-scale coastal embankment in the QE has been carried out for the purpose of flood defense, land requirements, etc.. Up to date, more than 1000 km^2 land has been reclaimed and the width of the estuary has been largely narrowed, especially at the middle reach, i.e., between Zakou and Ganpu (Fig. 1a).

3. Data and analysis

The bathymetry in this reach has been investigated in every April, July and November since the 1980s, representing the periods before and after flood season and low river discharge of the year. During each bathymetric investigation, the bed elevation along 60 cross-sections covering the middle Qiantang Estuary was observed using an Odom Hydrotrac echo-sounder. The error of the measured bed level is 0.1 m, and a global positioning system (GPS) by Trimble was used that gave the positioning error within 1 m. After each investigation, the volumes below multi-year averaged high water level (MHL) between the cross-sections were calculated. In this contribution, we collect the volume data of the sections Zakou-Yanguan (ZY) and

Yanguan-Ganpu (YG), as well as the monthly river discharge from FPS since 1981, in order to provide a comprehensive picture of the inter-annual and seasonal changes of the inside bar.

A detailed hydrographical survey was conducted during 9-17th October, 2015, at YG01 station located at the Yanguan section, where the tidal bore is strongest (Fig.1a). The flow velocity was measured by an Acoustic Doppler Current Profiler (ADCP), and SSC was measured using an Optical Back Scatter (OBS). The OBS instrument was calibrated against water samples collected at the same site. Because both flow velocity and SSC increase drastically at the bore arrival, the records was at one minute intervals in the hour around the bore arrival, and half an hour in the rest of the tidal period. No extreme conditions like flood events or storms occurred during the survey.

Furthermore, the daily river discharge from FPS and the detailed bathymetrical data in April, July and November in 2015 at the Zakou-Ganpu reach, were collected in order to relate the short-term hydrodynamics to long-term bathymetrical changes. The digital elevation models (DEM) were reconstructed by interpolation of the data using the Surfer software package, making use of the Kriging interpolation technique, which has been widely used in previous studies (e.g. van der Wal and Pye, 2002; Blott et al., 2006; Dai et al., 2014). Spatial deposition and erosion patterns and associated volume changes were calculated by subtraction of the DEMs.

4. Results

The volumes of ZY and YG sections are characterized by seasonal and inter-annual variations (Figs. 2a and 2b). Over ZY section, the volume in July is apparently larger than that in

April, and the volume in November is clearly smaller than in July and a little larger than in April. The mean values since 1981 in April, July and November are 294, 364 and 312×10^6 m^3, respectively. Moreover, the volumes in wet years (1987-1999 and 2010-2016) are larger than in dry years (1981-1986 and 2003-2009), by about 1.5 times on average. The volume in July at the ZY section correlates well with the mean river discharge during April-July (Fig. 2c):

$$V = 7.57Q^{0.54} \qquad (1)$$

in which V is volume in 10^6 m^3, Q is river discharge in m^3/s. The correlation coefficient is 0.91, indicating the river flow dominance on the morphology during the high discharge season.

The volume over the YG section has a decreasing trend which is related to the large-scale embankment in the Qiantang Estuary in the last decades (Xie et al., 2017b). Overall, the seasonal variation of the volume at YG section is opposite to that of ZY section, with the mean volumes 3304, 3173 and 3285×10^6 m^3, in April, July and November respectively, indicating the active sediment exchange between the two sections. The maximum volume change in the wet season of 1995 over ZY and YG sections can be 200 and 400×10^6 m^3, respectively. It should be noted that the volume changes of the ZY and YG sections are not always comparable because there exists active sediment exchange between the YG section and the lower estuary, i.e., the Hangzhou Bay (Chen et al., 1990; Han et al., 2003; Xie et al., 2017b).

The hydrodynamics at YG01 station during spring and intermediate tides in October 2015 were characterized by the tidal bore (Fig. 3). Upon the arrival of the bore, the water level increased by about 3 m within one minute. The velocity reversed from ebb current of less than

1.5 m/s to flood currents of 2.7 m/s in one minute and the maximum of 4.2 m/s was reached within half an hour. The SSC increased from less than 2 to about 15 kg/m^3 and the sediment flux reversed from less than 60 kg/s/m seawards to more than 300 kg/s/m landwards. The sediment fluxes during ebb tides were comparable to that of the adjacent Changjiang Estuary, which is normally less than 50 kg/s/m (Milliman et al., 1985; Su and Wang, 1986; Li et al., 2011); but the sediment fluxes under the tidal bore were clearly much larger than that of Changjiang Estuary, because of the large current velocity and associated SSC. During neap tides, undular bores were present and the capacity of sediment transport decreased significantly. The flood and ebb sediment fluxes were large, being about 900 t and 500 t per m during spring tides, respectively. The sediment fluxes during flood or ebb tides correlated well with the tidal range at Ganpu (Fig.3c). Overall, the net sediment transport was distinctly directed landward during spring and intermediate tides, whereas it was seaward during neap tides. In the spring-neap tidal cycle, the net landward sediment flux per m width was about 2000 t, indicating distinct accretion would occur in the dry season.

Figs. 4a and 4b illustrate the erosion and deposition patterns during April-July and July-November, 2015. Only one river flood event occurred in June, with the peak discharge being 12.600 m^3/s (Fig. 4c). Overall, the bed level changes were consistent with the numerical model of Xie et al (2017a) that during high flow, the upper part was eroded whereas the lower part was deposited. Clearly, the measured bathymetries provide more information on the spatial distribution of bed level changes. Despite the short duration of the river flood (about 10 days), the bed upstream of Yanguan was seriously eroded. The erosion mainly occurred around the thalweg, and the maximum erosion was more than 5 m. The volume over ZY section increased from 301×10^6 to 424×10^6 m^3, indicating an erosion of 123×10^6 m^3. The eroded sediment was transported seaward and deposited in the reach downwards of Yanguan, i.e., YG section and the Hangzhou Bay. The volume over YG section decreased from 2762×10^6 to 2692×10^6 m^3, indicating a decrease of 70×10^6 m^3. The bed level changes from July to November were opposite:sedimentation of 46×10^6 m^3 at ZY section and erosion of 25×10^6 m^3 at YG section.

Assuming that the observed data during October 2015 can represent the period between July and November, and considering that the width at Yanguan section is about 2.5 km, the cumulative landward sediment transport from July to November was about 80×10^6 t. Given that the dry density of the sediment is 1650 kg/m^3, the net sedimentation was about 48×10^6 m^3, consistent with the volume change based on the DEM comparison.

5. Discussion and conclusions

Results in this study support the conceptual model of Hoitink et al (2017) who proposed that seasonal variations of river flow can play an important role on the estuarine morphodynamic equilibrium. Under usual flow discharge conditions, sediment transport is directed landwards. The role of the big tidal bore on the landward sediment transport is not intrinsically different from the flood dominance in other estuaries (Dronkers, 1986; Wang et al., 2002; Bolle et al., 2010). On the other hand, the capacity of sediment transport of the bore is much larger than normal tidal currents. The flood current velocities during spring and intermediate tides can be more than 4 m/s, about twice of the maximum velocity of ebb tides, which results in extreme flood dominance. Furthermore, the sediment in the estuary is composed of silt and clay that can be easily resuspended and transported, with a critical velocity for erosion of 0.3-0.4 m/s (Chien et al., 1964; Han et al., 2003). When the bore arrives, SSC also increases drastically and hence the sediment flux per unit width during flood tides is very large, up to 300 kg/s/m. Whereas the current velocity and SSC during ebb tides are much less, and the sediment flux during ebb is less despite the much longer ebb duration. As a result, the net sediment transport over a tidal cycle is directed landward. The river flood events produce remarkable erosion. The larger the river discharge, the more sediment can be transported seaward. In a seasonal timescale, the morphology in the estuary is apparently deviated from its equilibrium; but within a whole year, the two opposite processes can be balanced and subsequently a dynamic equilibrium can be maintained.

One of the most striking features of Qiantang Estuary is bed erosion during river flood events, especially in the upper reach of the estuary (Fig. 4b). The serious bed degradation can be explained by the fact that the discharge during a river flood event is much larger than the normal discharge which is around 1000 m^3/s (Chen et al., 2006; Xie et al., 2017a). In previous studies, the cross-sectional area and the cross-sectionally averaged depth, have been found as a power function of the river discharge (Leopold and Maddock, 1953; Smith, 1974; Han et al., 2009). Considering that the volume is a function of cross-sectional area and the length, it is reasonable that the volume adjusts in a power relation with the changes of river discharge, as fitted by Eq.(1). Such formula provides a simple tool to predict the bathymetry of the estuary, given the river discharge is available.

In general, river flood induces active channel morphodynamics such as bank erosion and point bar deposition due to increased discharge and enhanced sediment concentrations (e.g. Mutti et al., 1985; Dalrymple and Choi, 2007). However, such channel morphodynamics is apparently not the case in the present Qiantang Estuary. Instead, the bed level rises and falls in response to sediment import and export. This is because the estuary has been significantly influenced by human intervention such as coastal embankments and the construction of unerodible artificial levee (Fig. 1a). Actually, before the large-scale embankment in the estuary, pronounced lateral migration of the thalweg occurred frequently, especially at the bends like Qibao and Jianshan (Chien et al., 1964). This is mainly caused by the inconsistence of flood and ebb current routes, which would adjust according to the seasonal changes of the relative strength of river flow to tidal current.

6. Conclusions

The big dataset obtained from long-term bathymetry and hydrological survey in the Qiantang Estuary provided a quantitative illustration of how a dynamic equilibrium is maintained over a seasonal and inter-annual scale. The active morphological behaviors are controlled by river flood events and the extreme flood dominance (the tidal bore). The tidal bore transports a large amount of sediment landward, causing accumulation during normal river discharge periods. Conversely, river flood events erode the bed severely. Furthermore, a power function was built between the averaged river discharge in high flow season and the channel volume of the upper part. The estuary has also been significantly influenced by the large-scale embankment in last decades, which constrained the lateral migration of thalweg and point bar deposition.

Acknowledgements

This research was supported by the National Natural Science Foundation of China [Grant number 41676085]; Zhejiang Provincial Natural Science Foundation of China [Grant number LY16D060004].

References

Bartsch-Winkler, S., Lynch, D.K., 1988. Catalog of worldwide tidal bore occurrences and Characteristics. USGS Circular, 1022, pp. l-17.

Bolle, A., Wang, Z.B., Amos, C., De Ronde, J., 2010.The influence of changes in tidal asymmetry on residual sediment transport in the Western Scheldt. Cont. Shelf Res., 30(8), 871-882.

Chanson, H., 2012, Tidal bores, Aegir, Eagre, Mascaret, Pororoca: Theory and observations: World Science., Singapore.

Blott, S.J., Pye, K., van der Wal, D., Neal, A., 2006. Long-term morphological change and its causes in the Mersey Estuary, NW England. Geomorphology, 81 (1-2), 185-206.

Bolla Pittaluga, M., Tambroni, N., Canestrelli, A., Slingerland, R., Lanzoni, S., Seminara ,G., 2015. Where river and tide meet: The morphodynamic equilibrium of alluvial estuaries, J. Geophys. Res. Earth Surf., 120, 75-94.

Chen, J.Y., Liu, C.Z., Zhang, C.L., Walker, H.J., 1990. Geomorphological development and sedimentation in Qiantang Estuary and Hangzhou Bay. J. Coast. Res., 6, 559-572.

Chen, S. M., Han, Z. C., Hu, G. J., 2006. Impact of human activities on the river reach in the Qiantang Estuary. J. Sediment. Res., 4, 61-67 (in Chinese with English abstract).

Chien, N., Sie, H.S., Chow, C.T., Lee Q.P., 1964. The fluvial processes of the big sand bar inside the Chien Tang Chiang Estuary. Acta Geograph. Sin., 30(2), 124-142 (in Chinese with English abstract).

Cooper, J.A.G., 1993. Sedimentation in a river dominated estuary. Sedimentology, 40, 979-1017.

Dai, Z.J., Liu, J.T., Xie, H.L., Shi, W.Y., 2014. Sedimentation in the outer Hangzhou Bay, China: the influence of Changjiang sediment load. J. Coast. Res., 30, 1218-1225.

Dalrymple, R.W., Choi, K., 2007. Morphologic and facies trends through the fluvial-marine transition in tide-dominated depositional systems: a schematic framework for environmental and sequence-stratigraphic interpretation. Earth Sci. Rev., 81, 135-174.

Dronkers, J., 1986. Tidal asymmetry and estuarine morphology. Nether. J. Sea. Res., 20(2/3), 117-131.

Dyer, K.R., 1995. Sediment transport processes in estuaries. In: Perillo, G.M.E. (Ed.), Geomorphology and sedimentology of Estuaries. Elsev. Sci. Pub., Amsterdam, pp. 423-449.

Fairbridge, R.W., 1980. The estuary: its definition and geodynamic cycle. In: Olausson, E., Cato, I. (Eds.), Chemistry and biogeochemistry of estuaries. John Wiley & Sons, New York, pp. 1-36.

Gao, S., Collins, M. B., 2014. Holocene sedimentary systems on continental shelves. Mar. Geol., 352, 268-294.

Han Z.C., Cao, Y., You, A.J., 2009. Verification of fluvio morphology for macro-tide estuary with tidal bore. Hydro-Sci. Eng., (4), 83-91 (in Chinese with English abstract).

Han, Z.C., Dai, Z.H., Li, G.B., 2003. Regulation and Exploitation of Qiantang Estuary. China Water Power Press, Beijing (in Chinese).

Hibma, A., Stive, M.J.F., Wang, Z.B., 2004. Esturine morphodynamics. Coast. Eng. 51, 765-778.

Hoitink, A.J.F., Wang, Z.B., Vermeulen, B., Huismans, Y., Kästner, K., 2017. Tidal controls on river delta morphology. Nature Geosci., 10, 637-645.

Lanzoni, S., Seminara, G., 2002. Long term evolution and morphodynamic equilibrium of tidal channels. J. Geophys. Res., 107, 3001.

Leopold, L.B., Maddock, T., 1953. The hydraulic geometry of stream channels and some physiographic implications. USGS Prof. Pap., pp. 252

Li, M. T., Chen, Z.Y., Yin, D.W., Chen, J., Wang, Z.H., Sun, Q.L., 2011. Morphodynamic characteristics of the dextral diversion of the Yangtze River mouth, China: Tidal and the Coriolis Force controls. Earth Surf. Processes Landforms, 36(5), 641-650.

Milliman, J.D., Shen, H.T., Tang, Z.S., Meade, R.H., 1985. Transport and deposition of river sediment in the Changjiang estuary and adjacent continental shelf. Cont. Shelf Res., 4, 37-45.

Mutti, E., Rosell, J., Allen, G.P., Fonnesu, F., Sgavetti, M., 1985. The Eocene Baronia tide dominated delta-shelf system in the Ager Basin. In: Mila, M.D., Rosell, J. (Eds.), Excursion Guidebook, 6th European Regional Meeting. Inter. Assoc. Sediment., Lleida, Spain, pp. 579-600.

Pan C.H., Lin, B.Y., Mao, X.Z., 2007. Case study: Numerical modeling of the tidal bore on the Qiantang River, China. J. Hydrau. Eng., 133, 130-138.

Pye, K., Blott, S.J., 2014. The geomorphology of UK estuaries: The role of geological controls, antecedent conditions and human activities. Estu., Coast. Shelf Sci., 150, 196-214.

Smith, T.R., 1974. A derivation of the hydraulic geometry of steady-state channels from conservation principles and sediment transport laws. J. Geol., 82(1), 98-104.

Su, J.L., Wang, K.S., 1986. The suspended sediment balance in Changjiang Estuary. Estu., Coast.

Shelf Sci., 23, 81-98.

van der Wal, D., Pye, K., Neal, A., 2002. Long-term morphological change in the Ribble Estuary, northwest England. Mar. Geol., 189, 249-266.

van der Wegen, M., Roelvink, J.A., 2008. Long-term morphodynamic evolution of a tidal embayment using a two-dimensional, process-based model. J. Geophys. Res., 113, C03016.

Wang, Z.B., Jeuken, M.C.J.L., Gerritsen, H., De Vriend, H.J., Kornman, B.A., 2002. Morphology and asymmetry of the vertical tide in the Westerschelde estuary. Cont. Shelf Res., 22, 2599-2609.

Xie, D.F., Gao, S., Wang, Z.B., Pan, C.H., Wu, X.G., Wang, Q.S., 2017a. Morphodynamic modeling of a large inside sandbar and its dextral morphology in a convergent estuary: Qiantang Estuary, China. J. Geophys. Res.: Earth Surf., 122, 1553-157.

Xie, D.F., Pan, C.H., Wu, X.G., Gao, S., Wang, Z.B., 2017b. Local human activities overwhelm decreased sediment supply from the Changjiang River: Continued rapid accumulation in the Hangzhou Bay - Qiantang Estuary system. Mar. Geol., 392, 66-77.

Yu, Q., Wang, Y.W., Gao, S., Flemming, B., 2012. Modeling the formation of a sand bar within a large funnel-shaped, tide-dominated estuary: Qiantangjiang Estuary, China. Mar. Geol., 299-302, 63-76.

Zhang, M., Townend, I., Zhou, Y., Cai, H., 2016. Seasonal variation of river and tide energy in the Yangtze estuary, China. Earth Surf. Proc. Landform., 41(1), 98-116.

FIGURE CAPTIONS

Fig.1. (a) Location of the Qiantang Estuary, in which YG01 denotes the hydrographic observation station in October, 2015. (b) The lateral-averaged longitudinal bathymetry along the estuary measured in 2014. (c) Bathymetry of the estuary measured in April, 2015. Fig. 1a and 1b were modified from Xie et al., 2017a.

Fig. 2. (a, b) The volumes of ZY and YG sections in every April, July and November since 1981. The shades denote the continuous dry years. (c) Relationship between the volume of ZY section in July and the average river discharge from April to July. Data in April of Fig. 2A and 2B from Xie et al. (2017b).

Fig. 3. (a, b) Time series of tidal level, depth-averaged current velocity, SSC and sediment flux at YG01 station during 9-17th October, 2015. (c) Relationship between flood and ebb sediment fluxes and tidal range at Ganpu station. (d) The cumulative and net sediment fluxes during the measurement.

Fig. 4. (a, b) Bed erosion and accretion patterns from April to July and from July to November in 2015. (c) Time series of daily river discharge from FPS in 2015.

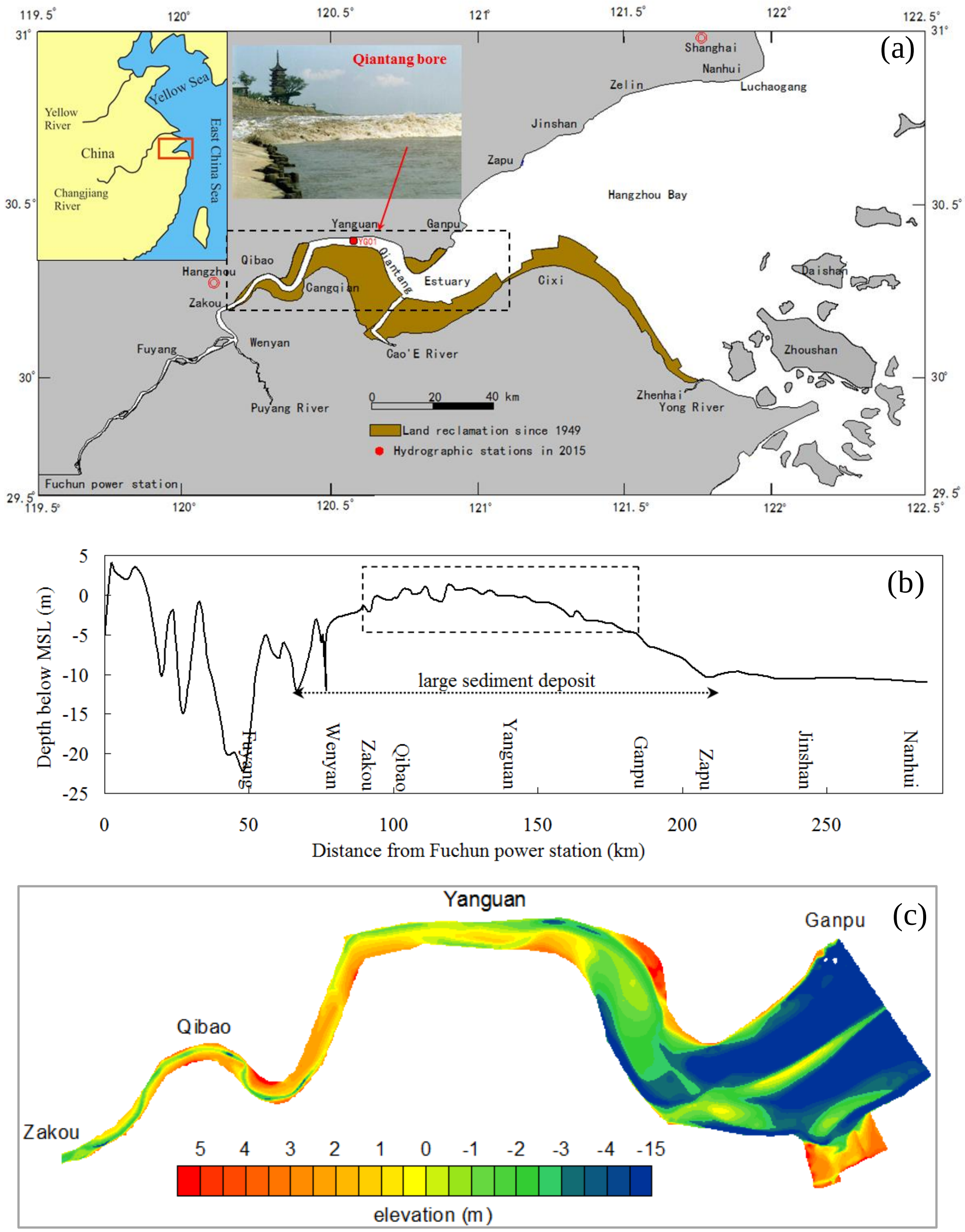

(a)
Qiantang bore
Yellow Sea
East China Sea
Yellow River
China
Changjiang River
Shanghai
Nanhui
Luchaogang
Zelin
Jinshan
Zapu
Hangzhou Bay
Ganpu
Yanguan
YG01
Qibao
Hangzhou
Zakou
Cangqian
Qiantang
Estuary
Cixi
Daishan
Zhoushan
Fuyang
Wenyan
Cao'E River
Puyang River
Zhenhai
Yong River
Fuchun power station
0 20 40 km
Land reclamation since 1949
Hydrographic stations in 2015
(b)
Depth below MSL (m)
large sediment deposit
Fuyang
Wenyan
Zakou
Qibao
Yanguan
Ganpu
Zapu
Jinshan
Nanhui
Distance from Fuchun power station (km)
(c)
Yanguan
Ganpu
Qibao
Zakou
elevation (m)

Fig. 1.

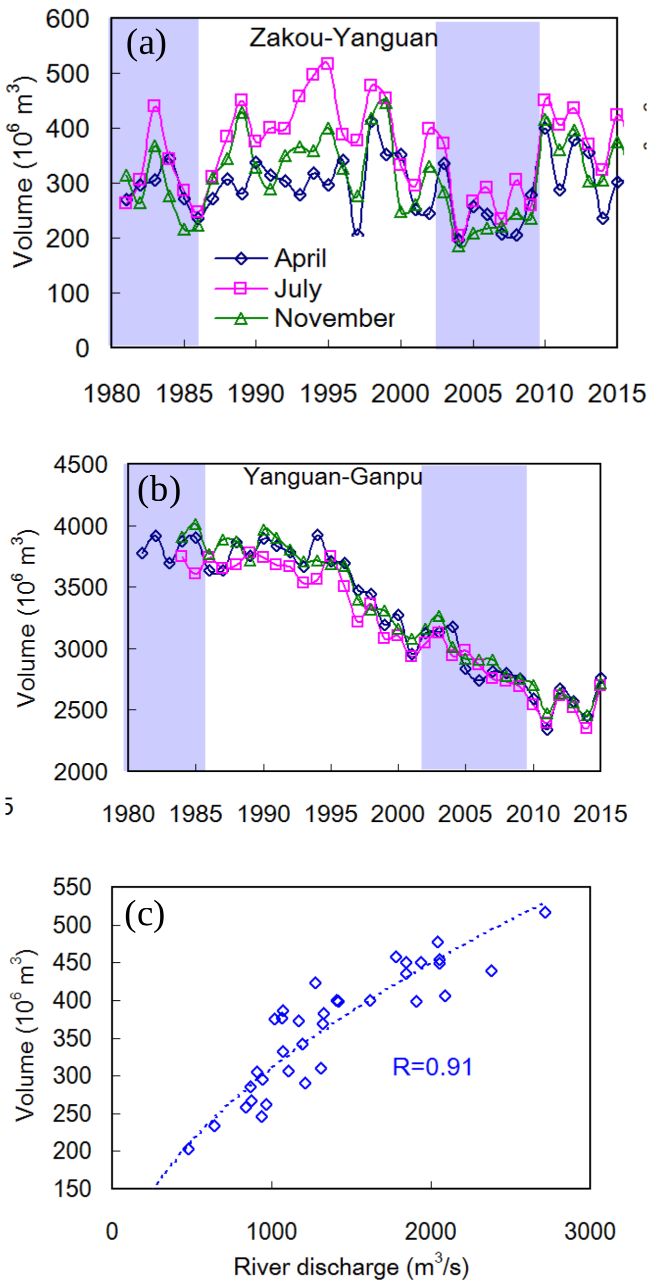
(a)
Zakou-Yanguan
Volume (10^6 m^3)
April
July
November
600
500
400
300
200
100
0
1980
1985
1990
1995
2000
2005
2010
2015
(b)
Yanguan-Ganpu
Volume (10^6 m^3)
4500
4000
3500
3000
2500
2000
1980
1985
1990
1995
2000
2005
2010
2015
(c)
R=0.91
Volume (10^6 m^3)
River discharge (m^3/s)
550
500
450
400
350
300
250
200
150
0
1000
2000
3000

Fig. 2.

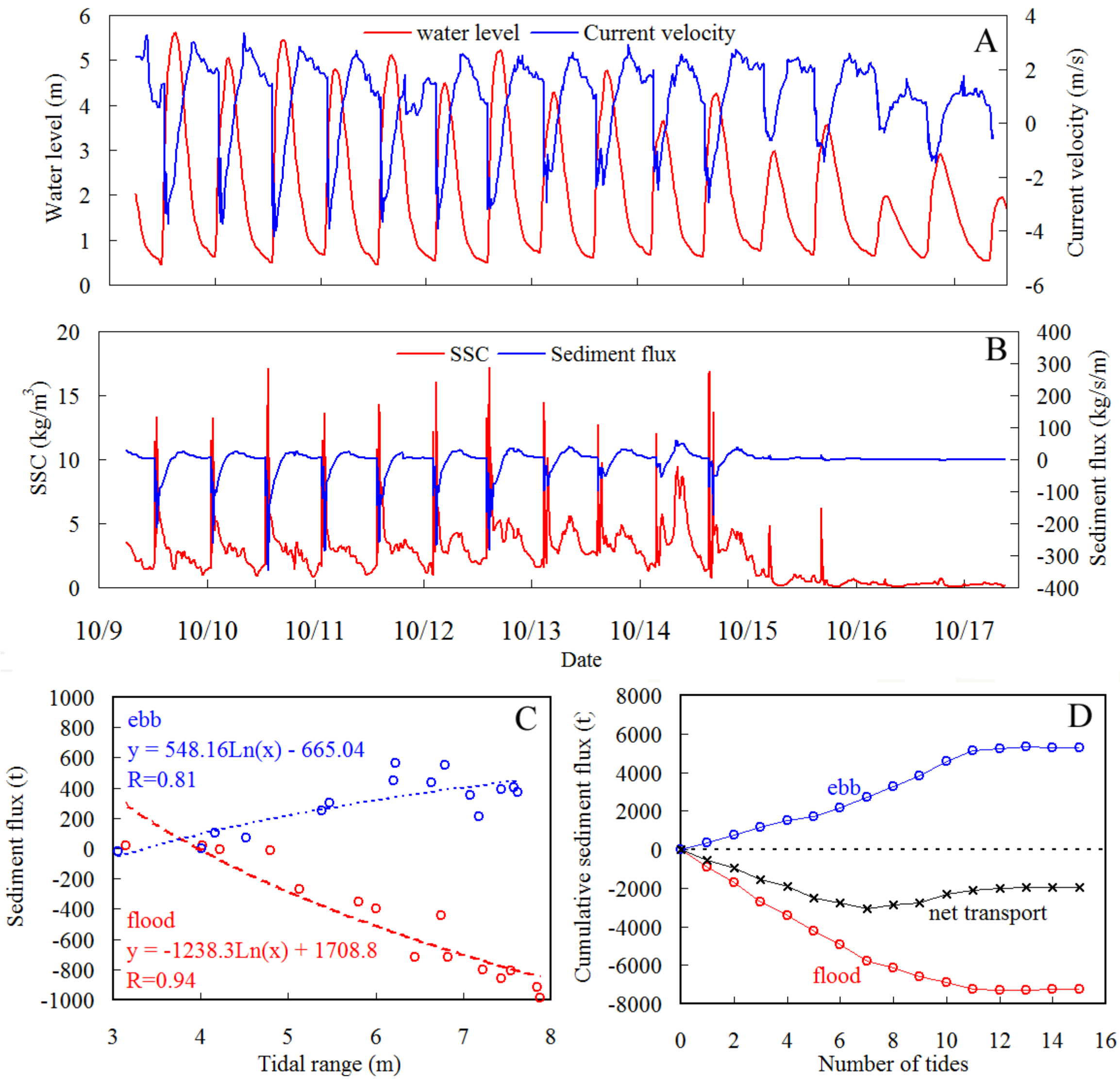
water level
Current velocity
A
Water level (m)
Current velocity (m/s)
SSC
Sediment flux
B
SSC (kg/m^3)
Sediment flux (kg/s/m)
10/9
10/10
10/11
10/12
10/13
10/14
10/15
10/16
10/17
Date
C
ebb
y = 548.16Ln(x) - 665.04
R=0.81
flood
y = -1238.3Ln(x) + 1708.8
R=0.94
Sediment flux (t)
Tidal range (m)
D
ebb
net transport
flood
Cumulative sediment flux (t)
Number of tides

Fig. 3.

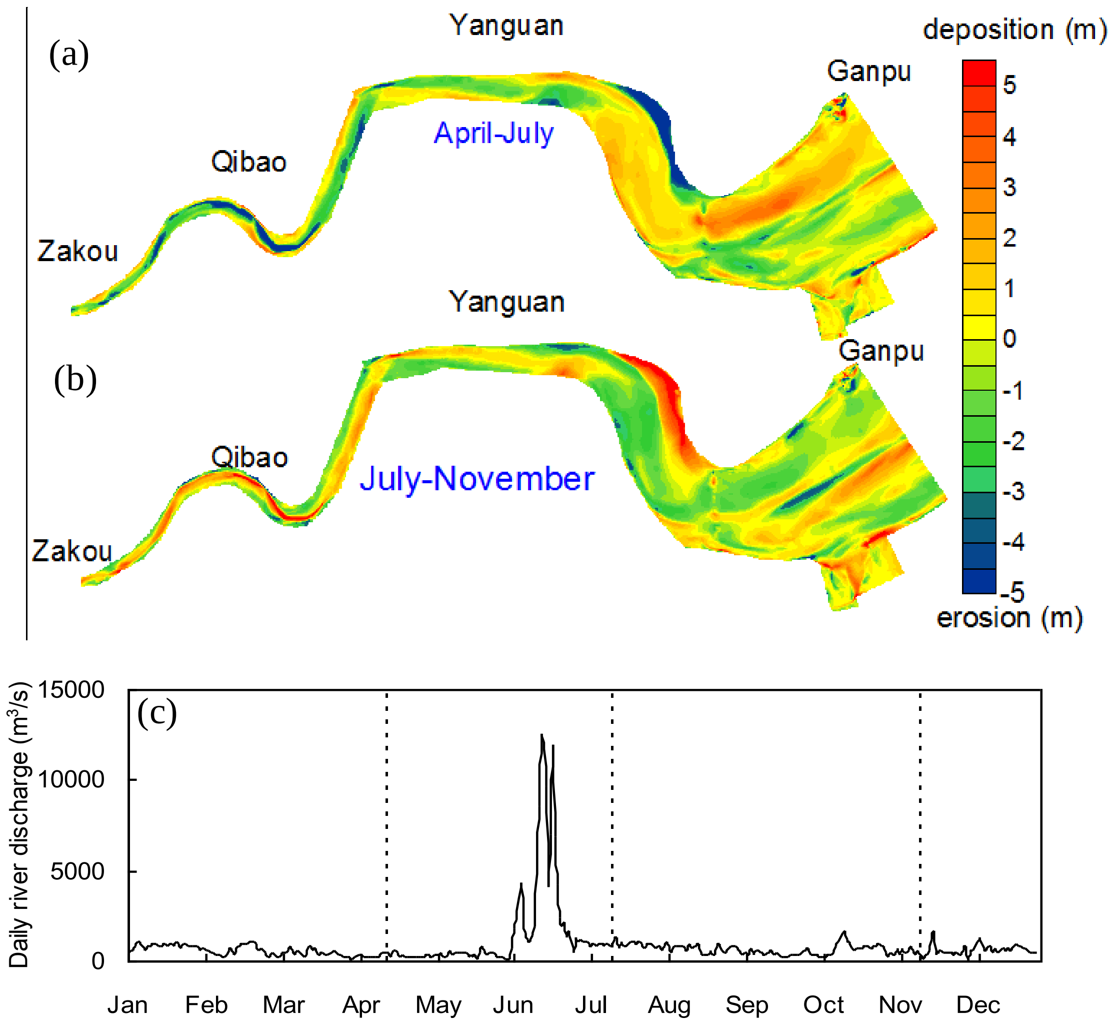
(a)
Yanguan
Qibao
Zakou
Ganpu
April-July
(b)
Yanguan
Qibao
Zakou
Ganpu
July-November
deposition (m)
5
4
3
2
1
0
-1
-2
-3
-4
-5
erosion (m)
(c)
Daily river discharge (m³/s)
15000
10000
5000
0
Jan
Feb
Mar
Apr
May
Jun
Jul
Aug
Sep
Oct
Nov
Dec

Fig. 4.